

The quantum transmitting boundary method

Craig S. Lent, and David J. Kirkner

Citation: [Journal of Applied Physics](#) **67**, 6353 (1990); doi: 10.1063/1.345156

View online: <https://doi.org/10.1063/1.345156>

View Table of Contents: <http://aip.scitation.org/toc/jap/67/10>

Published by the [American Institute of Physics](#)

Articles you may be interested in

[Quantum transmitting boundary method in a magnetic field](#)

[Journal of Applied Physics](#) **76**, 2240 (1994); 10.1063/1.357642

[Single and multiband modeling of quantum electron transport through layered semiconductor devices](#)

[Journal of Applied Physics](#) **81**, 7845 (1997); 10.1063/1.365394

[A self-consistent solution of Schrödinger–Poisson equations using a nonuniform mesh](#)

[Journal of Applied Physics](#) **68**, 4071 (1990); 10.1063/1.346245

[Tunneling in a finite superlattice](#)

[Applied Physics Letters](#) **22**, 562 (1973); 10.1063/1.1654509

[Iteration scheme for the solution of the two-dimensional Schrödinger-Poisson equations in quantum structures](#)

[Journal of Applied Physics](#) **81**, 7880 (1997); 10.1063/1.365396

[An eigenvalue method for open-boundary quantum transmission problems](#)

[Journal of Applied Physics](#) **78**, 2177 (1995); 10.1063/1.360132

AIP | Journal of
Applied Physics

SPECIAL TOPICS



The quantum transmitting boundary method

Craig S. Lent

*Department of Electrical and Computer Engineering, University of Notre Dame,
Notre Dame, Indiana 46556*

David J. Kirkner

Department of Civil Engineering, University of Notre Dame, Notre Dame, Indiana 46556

(Received 13 December 1989; accepted for publication 30 January 1990)

A numerical algorithm for the solution of the two-dimensional effective mass Schrödinger equation for current-carrying states is developed. Boundary conditions appropriate for such states are developed and a solution algorithm constructed that is based on the finite element method. The utility of the technique is illustrated by solving problems relevant to submicron semiconductor quantum device structures.

I. INTRODUCTION

Recent advances in submicron lithography have made it possible to create very small structures in which electrons in the two-dimensional electron gas formed at a semiconductor heterostructure interface are further confined by metal gates. A negative voltage applied to the gate depletes electrons in the region beneath the gate. Several device structures have been proposed and realized using this scheme.¹⁻⁵ For sufficiently small scales, electrons in such structures are ballistic and coherent over the entire device region. For many purposes, electronic transport in this regime is governed by the effective-mass Schrödinger equation. Understanding and modeling the performance of these device structures requires solving the two-dimensional Schrödinger equation.

Several well-established techniques have been employed for obtaining numerical solutions of the two-dimensional Schrödinger equation for bound states. Bound-state solutions, however, are not of primary interest in understanding quantum devices. States which carry current, sometimes called "scattering states" are more important in understanding current flow through small coherent regions. In one dimension, the current carrying states can be solved for rather straightforwardly because the Schrödinger equation can be simply integrated from one side of the device to the other. In two dimensions the problem is more difficult.

Current-carrying states are composed of solutions in a device region (the scattering region) and solutions that extend to infinity along the input and output leads. Because of the regularity of the potential in the leads, the form of the solution is known in the lead regions. This can usually be expressed as a sum of traveling and evanescent modes in the leads. The complex amplitudes of each of these modes is unknown, however. The amplitudes are a result of the problem's solutions, commonly expressed in terms of transmission and reflection coefficients. Therefore, although the asymptotic form of the solution may be known, the values of the wave function and its derivative on a boundary region are only known in terms of coefficients which are to be determined. Numerical solution requires knowledge of the wave function or its derivative on some boundary region. In one dimension, this boundary value problem can be treated as an initial value problem using Numerov-type methods. In two dimensions it cannot.

We formulate the boundary conditions appropriate for the numerical solution of the Schrödinger equation for current-carrying states on a two-dimensional domain. We employ these boundary conditions in developing a numerical solution algorithm based on the finite element method. We call this the quantum transmitting boundary method (QTBM). In Ref. 6, we formulated the technique for the rather restricted case of two colinear leads with infinite square-well cross sections and identical widths. Here we develop the completely general formulation, capable of solving the general problem of the transmission and reflection properties of a region with an arbitrary potential, including multiple multimoded input leads of arbitrary cross section and orientation. The QTBM yields not only the transmission and reflection coefficients, but the full wave function in the device region.

Section II contains the formal statement of the problem and the development of the boundary conditions for each lead. This section is quite general and does not depend on any particular numerical technique. The numerical algorithm is developed in Sec. III. Section III C contains a description of the basic features of the QTBM algorithm and a comparison with other techniques. In Sec. IV we present a few short examples of the application of the QTBM to some interesting geometries for quantum structures. Section V states our conclusions.

II. FORMULATION OF THE BOUNDARY CONDITIONS

A. Problem statement

The region of interest is partitioned into a "device" region Ω_0 , and several lead regions, $\Omega_1, \Omega_2, \dots, \Omega_n$, which extend to infinity. We want to solve the two-dimensional effective-mass Schrödinger equation on $\Omega \equiv \Omega_0 \cup \Omega_1 \cup \Omega_2 \dots \cup \Omega_n$. The boundary of the region Ω_0 we denote Γ . The boundary between a lead region, Ω_i , and the device region, Ω_0 , we call Γ_i . This lead boundary can, without loss of generality, be taken to be a straight line. The rest of the boundary Γ , which is not a lead boundary, is denoted Γ_0 (see Fig. 1).

The problem we wish to solve can be stated as follows:

Given: The total energy E , the potential energy in each region, $V_i(x, y)$, $i = 0, 1, 2, \dots, n$, and the complex amplitudes of each incoming mode in each lead,

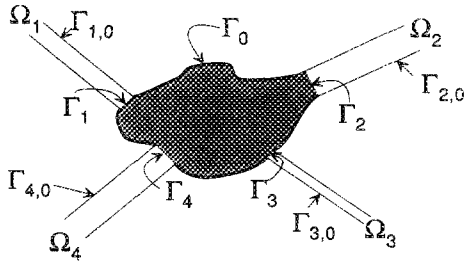


FIG. 1. The problem geometry.

Find:

$$\psi_0 \in C^2(\Omega_0), \psi_i \in C^2(\Omega_i), \dots, \text{ and } \psi_n \in C^2(\Omega_n),$$

such that

$$-(\hbar^2/2m^*)\nabla^2\psi_i(x,y) + V_i(x,y)\psi_i(x,y) = E\psi_i(x,y), \quad (x,y) \in \Omega_i, \quad (1)$$

and

$$\psi_0 = \psi_i \text{ on } \Gamma_i, \quad (2)$$

$$\nabla\psi_0 \cdot \hat{n}_{\Gamma_i} = \nabla\psi_i \cdot \hat{n}_{\Gamma_i} \text{ on } \Gamma_i, \quad (3)$$

$$\psi_0 = 0 \text{ on } \Gamma_0 \equiv \partial\Omega_0 - \sum_i \Gamma_i, \quad (4)$$

$$\psi_i = 0 \text{ on } \Gamma_0 \equiv \partial\Omega_i - \Gamma_i, \quad (5)$$

$$\psi_i \text{ bounded as } \sqrt{x^2 + y^2} \rightarrow \infty. \quad (6)$$

We will develop a solution algorithm valid for any potential $V_0(x, y)$ in the device region. The condition that ψ_0 vanish on the boundary Γ_0 need not be restrictive in that the boundary can always be placed far enough from the active device region that the wave function has vanishingly small amplitude on the boundary. The device region must, in this sense, contain the wave function within Ω_0 except along the lead boundaries.

We require that the potential $V_i(x, y)$ in each lead be independent of the distance along the lead. This is what we mean by leads—channels that contain no longitudinal structure, although they may have a complicated cross section. In the next section we consider the form of the solutions in the leads themselves. Our goal is to formulate a boundary condition on the lead boundaries Γ_i that will allow us to specify the incoming flux in each lead and solve the Schrödinger equation only in the device region Ω_0 .

B. Solution in the leads

By requiring the leads to be uniform along their lengths we can separate the problem in the lead regions into coupled one-dimensional problems. We define a local coordinate system in each lead i ,

$$(\eta_i, \xi_i) = [\eta_i(x, y), \xi_i(x, y)], \quad (7)$$

such that $\hat{\eta}_i$ is parallel to the lead walls and points down the lead in the direction away from Ω_0 (see Fig. 2). The $\hat{\xi}_i$ direction is perpendicular to $\hat{\eta}_i$ and the boundary between Ω_i and Ω_0 can be written

$$\Gamma_i = \{(\eta_i, \xi_i) | \xi_i \in (0, d_i), \eta_i = 0\}. \quad (8)$$

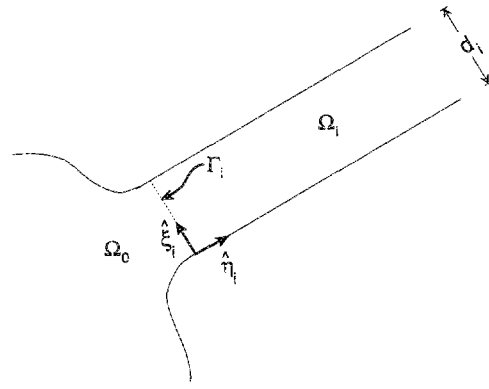


FIG. 2. Local coordinate system for lead i .

Here d_i is the perpendicular width of the lead. The potential in the lead is assumed to vary only across the lead:

$$V_i(\eta_i, \xi_i) = V_i(\xi_i). \quad (9)$$

For the simple case of square-well leads, $V_i(\xi_i) = 0$.

Because the potential in the leads is independent of η , the Schrödinger equation in the leads separates and we can write the general solution in lead i as

$$\psi_i(\eta_i, \xi_i) = \sum_{m=1}^{N^i} a_m^i \chi_m^i(\xi_i) e^{-ik_m^i \eta_i} + b_m^i \chi_m^i(\xi_i) e^{ik_m^i \eta_i} + \sum_{m=N^i+1}^{\infty} b_m^i \chi_m^i(\xi_i) e^{-k_m^i \eta_i}, \quad (10)$$

where $\chi_m^i(\xi_i)$ is the m th eigenstate of the one-dimensional Schrödinger equation,

$$-(\hbar^2/2m^*)[\partial^2 \chi_m^i(\xi_i)/\partial \xi_i^2] + V_i(\xi_i)\chi_m^i(\xi_i) = E_m^i \chi_m^i(\xi_i). \quad (11)$$

The a_m^i 's are the coefficients of the incoming traveling-wave states and are an input to the problem. N^i is the number of traveling-wave modes allowed in lead i . The b_m^i 's in the first sum are the coefficients of outgoing traveling-wave states. The b_m^i 's in the second sum are coefficients of evanescent (exponentially decaying) states. The coefficients b_m^i are unknowns that must be calculated as part of the problem solution. We can choose the eigenstates χ to be orthonormal:

$$\int_0^{d_i} [\chi_m^i(\xi_i)]^* \chi_n^i(\xi_i) d\xi_i = \delta_{m,n}. \quad (12)$$

For infinite square-well leads,

$$\chi_m^i(\xi_i) = \sqrt{2/d_i} \sin[(m\pi/d)\xi_i]. \quad (13)$$

The wave vector for the m th mode in the i th lead is given by

$$k_m^i = \sqrt{|(2m^*/\hbar^2)(E - E_m^i)|}. \quad (14)$$

The number of traveling waves N^i is the maximum m such that $E > E_m^i$.

C. Boundary conditions at the lead interfaces

At the boundary between the device region and lead i we require both continuity of the wave function and the normal derivative [Eqs. (2) and (3)]. The condition on the deriva-

tive can be written

$$\begin{aligned}\nabla\psi_0(\mathbf{r})\cdot\hat{n}_{\Gamma_i} &= \nabla\psi_i(\mathbf{r})\cdot\hat{n}_{\Gamma_i} \text{ on } \Gamma_i \\ &= \frac{\partial}{\partial\eta_i}\psi_i(\eta_i,\xi_i)\Big|_{\eta_i=0}.\end{aligned}\quad (15)$$

We calculate the normal derivative from the known form of the wave function given by Eq. (10):

$$\begin{aligned}\frac{\partial\psi_i}{\partial\eta_i}\Big|_{\eta_i=0} &= \sum_{m=1}^{N^i} -ia_m^i k_m^i \chi_m^i(\xi_i) + ib_m^i k_m^i \chi_m^i(\xi_i) \\ &\quad - \sum_{m=N^i+1}^{\infty} k_m^i b_m^i \chi_m^i(\xi_i).\end{aligned}\quad (16)$$

We can evaluate the b_m^i 's by using the orthogonality of the χ 's at $\eta_i = 0$:

$$b_m^i = \int_0^{d_i} \chi_m^i(\xi_i) \psi_i(\eta_i=0, \xi_i) d\xi_i - a_m^i. \quad (17)$$

So

$$\begin{aligned}\frac{\partial\psi_i}{\partial\eta_i}\Big|_{\eta_i=0} &= \sum_{m=1}^N ik_m^i \chi_m^i(\xi_i) \\ &\quad \times \left(-2a_m^i + \int_0^{d_i} \chi_m^i(\xi_i) \psi_i(\eta_i=0, \xi_i) d\xi_i \right) \\ &\quad - \sum_{m=N+1}^{\infty} k_m^i \chi_m^i(\xi_i) \\ &\quad \times \left(\int_0^{d_i} \chi_m^i(\xi_i) \psi_i(\eta_i=0, \xi_i) d\xi_i \right).\end{aligned}\quad (18)$$

The derivative boundary condition then becomes

$$\begin{aligned}\nabla\psi_0(\mathbf{r})\cdot\hat{n}_{\Gamma_0} &= f_i[\xi_i, \psi_i(\eta_i=0, \xi_i)] \\ &= \sum_{m=1}^{N^i} ik_m^i \chi_m^i(\xi_i) \\ &\quad \times \left(-2a_m^i + \int_0^{d_i} \chi_m^i(\xi_i) \psi_i(\eta_i=0, \xi_i) d\xi_i \right) \\ &\quad - \sum_{m=N^i+1}^{\infty} k_m^i \chi_m^i(\xi_i) \\ &\quad \times \left(\int_0^{d_i} \chi_m^i(\xi_i) \psi_i(\eta_i=0, \xi_i) d\xi_i \right).\end{aligned}\quad (19)$$

We can now employ Eq. (2), the continuity of the wave function itself, and replace ψ_i 's on the right-hand side by ψ_0 's since they are evaluated only on the boundary. We then obtain a boundary condition on ψ_0 and its normal derivative:

$$\begin{aligned}\nabla\psi_0(\mathbf{r})\cdot\hat{n}_{\Gamma_0} &= f_i[\xi_i, \psi_0(\eta_i=0, \xi_i)] \\ &= \sum_{m=1}^{N^i} ik_m^i \chi_m^i(\xi_i) \\ &\quad \times \left(-2a_m^i + \int_0^{d_i} \chi_m^i(\xi_i) \psi_0(\eta_i=0, \xi_i) d\xi_i \right) \\ &\quad - \sum_{m=N^i+1}^{\infty} k_m^i \chi_m^i(\xi_i) \\ &\quad \times \left(\int_0^{d_i} \chi_m^i(\xi_i) \psi_0(\eta_i=0, \xi_i) d\xi_i \right).\end{aligned}\quad (20)$$

Equation (20) defines the functional f_i and is the boundary condition we require in order to formulate the problem for the current-carrying states as a boundary-value problem. Note that Eq. (20) relates the value of the wave function's normal derivative at a particular point to the values of the wave function at all the other points along the boundary.

D. Weak variational form of the Schrödinger equation

In this section we develop the weak variational form⁷ of the Schrödinger equation in a way suitable for numerical discretization. Our goal is to discretize the wave function only in the device region Ω_0 , and apply suitable boundary conditions to match wave function and derivative to the solution in the leads. We begin with the time-independent Schrödinger equation for the wave function ψ_0 in the device region:

$$-(\hbar^2/2m^*)\nabla^2\psi_0(x, y) + V(x, y)\psi_0(x, y) = E\psi_0(x, y). \quad (21)$$

This is multiplied by an arbitrary test function $\bar{\psi}$ and integrated over Ω_0 :

$$-\frac{\hbar^2}{2m^*} \int_{\Omega_0} \bar{\psi} \nabla^2 \psi_0 d^2r + \int_{\Omega_0} \bar{\psi} (V - E) \psi_0 d^2r = 0. \quad (22)$$

The test function is chosen so that it obeys the same essential boundary conditions as does ψ_0 , i.e., $\bar{\psi} = 0$ on Γ_0 .

Using Green's first identity we have,

$$\int_{\Omega} \phi \nabla^2 \psi d^2r = - \int_{\Omega} \nabla \phi \cdot \nabla \psi d^2r + \oint_{\Gamma} \phi (\nabla \psi \cdot \hat{n}_{\Gamma}) d\Gamma, \quad (23)$$

so the Schrödinger equation becomes

$$\begin{aligned}\frac{\hbar^2}{2m^*} \int_{\Omega_0} \nabla \bar{\psi} \cdot \nabla \psi_0 d^2r + \int_{\Omega_0} \bar{\psi} (V - E) \psi_0 d^2r \\ = \frac{\hbar^2}{2m^*} \oint_{\Gamma} \bar{\psi} (\nabla \psi_0 \cdot \hat{n}) d\Gamma.\end{aligned}\quad (24)$$

The integration around the boundary Γ must be performed in a counterclockwise direction. Since $\bar{\psi}$ is zero on Γ_0 , the right-hand side can be rewritten as an explicit sum over these contact regions:

$$\begin{aligned}\frac{\hbar^2}{2m^*} \int_{\Omega_0} \nabla \bar{\psi} \cdot \nabla \psi_0 d^2r + \int_{\Omega_0} \bar{\psi} (V - E) \psi_0 d^2r \\ = \frac{\hbar^2}{2m^*} \sum_i \int_{\Gamma_i} \bar{\psi} (\nabla \psi_0 \cdot \hat{n}) d\Gamma_i.\end{aligned}\quad (25)$$

E. The reformulated problem

The original problem statement can now be cast in the form of a weak variational statement with the boundary conditions given by Eq. (20). The geometry is the same illustrated in Fig. 1.

Given: The energy E , the potential energy $V(\mathbf{r})$, and the set $\{a_m^i\}$, where each a_m^i is the complex amplitude of the incoming wave in the m th mode of the i th lead,

Find: $\psi_0(\mathbf{r})$ for $\mathbf{r} \in \Omega_0$ such that

$$\frac{\hbar^2}{2m^*} \int_{\Omega_0} \nabla \bar{\psi} \cdot \nabla \psi_0 d^2r + \int_{\Omega_0} \bar{\psi} (V - E) \psi_0 d^2r = \frac{\hbar^2}{2m^*} \sum_i \int_{\Gamma_i} \bar{\psi} f_i[\xi_i, \psi_0] d\Gamma_i, \quad (26)$$

where

$$f_i[\xi_i, \psi_0] = \sum_{m=1}^{N^i} ik_m^i \chi_m^i(\xi_i) \times \left(-2a_m^i + \int_0^{d_i} \chi_m^i(\xi) \psi_0(\eta_i = 0, \xi_i) d\xi_i \right) - \sum_{m=N^i+1}^{\infty} k_m^i \chi_m^i(\xi_i) \times \left(\int_0^{d_i} \chi_m^i(\xi_i) \psi_0(\eta_i = 0, \xi_i) d\xi_i \right), \quad (27)$$

and $\bar{\psi}$ is an arbitrary test function which is zero on Γ_0 .

III. NUMERICAL SOLUTION

A. Finite element discretization

The discretization is on a mesh with m nodal points, $\mathbf{r}_1, \mathbf{r}_2, \dots, \mathbf{r}_m$. Associated with each nodal point, \mathbf{r}_i , is a global shape function $\phi_i(\mathbf{r})$ which has the property that

$$\phi_i(\mathbf{r}_j) = \delta_{ij}. \quad (28)$$

The wave function can be approximately expanded in the basis of these shape functions,

$$\psi_0(\mathbf{r}) = \sum_i \psi(\mathbf{r}_i) \phi_i(\mathbf{r}) = \sum_i u_i \phi_i(\mathbf{r}) \quad (29)$$

or

$$\psi_0(\mathbf{r}) = \mathbf{N}(\mathbf{r}) \cdot \mathbf{u}, \quad (30)$$

where $\mathbf{N}(\mathbf{r})$ is the $(1 \times m)$ matrix of global shape functions,

$$\mathbf{N}(\mathbf{r}) = [\phi_1(\mathbf{r}), \phi_2(\mathbf{r}), \phi_3(\mathbf{r}), \dots, \phi_m(\mathbf{r})], \quad (31)$$

and \mathbf{u} is the $(m \times 1)$ matrix of the (unknown) nodal values of ψ . Similarly, we can approximate the gradient of the wave function by an expansion on this basis set,

$$\nabla \psi_0(\mathbf{r}) = \left(\frac{\partial \psi_0}{\partial x}, \frac{\partial \psi_0}{\partial y} \right) = \mathbf{B}(\mathbf{r}) \cdot \mathbf{u}, \quad (32)$$

where

$$\mathbf{B}(\mathbf{r}) = \begin{pmatrix} \partial_x \phi_1(\mathbf{r}) & \partial_x \phi_2(\mathbf{r}) & \dots & \partial_x \phi_m(\mathbf{r}) \\ \partial_y \phi_1(\mathbf{r}) & \partial_y \phi_2(\mathbf{r}) & \dots & \partial_y \phi_m(\mathbf{r}) \end{pmatrix} \quad (33)$$

is the $(2 \times m)$ matrix of derivatives of the global shape functions.

We can make similar approximate expansions for the test function $\bar{\psi}$:

$$\bar{\psi} = \bar{\mathbf{u}}^T \cdot \mathbf{N}^T \quad (34)$$

$$\nabla \bar{\psi} = \bar{\mathbf{u}}^T \cdot \mathbf{B}^T, \quad (35)$$

where $\bar{\mathbf{u}}$ is the vector of nodal values of $\bar{\psi}$.

Inserting these approximate expansions into the Schrödinger equation yields,

$$\bar{\mathbf{u}}^T \left(\int_{\Omega_0} \frac{\hbar^2}{2m^*} \mathbf{B}^T(\mathbf{r}) \mathbf{B}(\mathbf{r}) d^2r \right) \mathbf{u} + \bar{\mathbf{u}}^T \times \left(\int_{\Omega_0} [V(\mathbf{r}) - E] \mathbf{N}^T(\mathbf{r}) \mathbf{N}(\mathbf{r}) d^2r \right) \mathbf{u} = \frac{\hbar^2}{2m^*} \sum_i \left(\int_{\Gamma_i} \bar{\psi}(\mathbf{r}) f_i[\xi_i, \psi_0(0, \xi_i)] d\Gamma_i \right). \quad (36)$$

For the moment we leave the right-hand side in an undiscretized form. We define the $(m \times m)$ matrices \mathbf{K} , \mathbf{T} , and \mathbf{V} as follows:

$$\mathbf{T} \equiv \int_{\Omega_0} \frac{\hbar^2}{2m^*} \mathbf{B}^T(\mathbf{r}) \mathbf{B}(\mathbf{r}) d^2r, \quad (37)$$

$$\mathbf{V} \equiv \int_{\Omega_0} [V(\mathbf{r}) - E] \mathbf{N}^T(\mathbf{r}) \mathbf{N}(\mathbf{r}) d^2r. \quad (38)$$

The (partially) discretized Schrödinger equation is then,

$$\bar{\mathbf{u}}^T (\mathbf{T} + \mathbf{V}) \mathbf{u} = \frac{\hbar^2}{2m^*} \sum_i \left(\int_{\Gamma_i} \bar{\psi}(\mathbf{r}) f_i[\xi_i, \psi_0(0, \xi_i)] d\Gamma_i \right). \quad (39)$$

The discretization of the right-hand-side boundary term proceeds as follows.

Let \mathbf{u}_i be the projection of \mathbf{u} onto Γ_i . Let the length of \mathbf{u}_i be M_i , the number of nodal points on the boundary (see Fig. 3). Let $\mathbf{N}_i(\xi_i)$ be the $(1 \times M_i)$ matrix of global shape functions, such that

$$\psi_0(\mathbf{r} \in \Gamma_i) = \psi_0(\eta_i = 0, \xi_i) = \mathbf{N}_i(\xi_i) \cdot \mathbf{u}_i. \quad (40)$$

Further, define a $(1 \times M_i)$ matrix $\mathbf{N}_{i,m}$ by

$$\mathbf{N}_{i,m} \equiv \int_0^{d_i} \chi_m^i(\xi_i) \mathbf{N}_i(\xi_i) d\xi_i. \quad (41)$$

The boundary term then can be written,

$$\begin{aligned} \frac{\hbar^2}{2m^*} \sum_i \left(\int_{\Gamma_i} \bar{\psi}(\mathbf{r}) f_i(\mathbf{r}, \mathbf{u}) d\Gamma_i \right) &= \frac{\hbar^2}{2m^*} \sum_i \bar{\mathbf{u}}^T \left[\sum_{m=1}^{N^i} -2ia_m^i k_m^i \int_0^{d_i} \mathbf{N}_i^T(\xi_i) \chi_m^i(\xi_i) d\xi_i \right. \\ &\quad + \sum_{m=1}^{N^i} ik_m^i \left(\int_0^{d_i} \mathbf{N}_i^T(\xi_i) \chi_m^i(\xi_i) d\xi_i \right) \left(\int_0^{d_i} \mathbf{N}_i(\xi_i) \chi_m^i(\xi_i) d\xi_i \right) \mathbf{u}_i \\ &\quad \left. - \sum_{m=N^i+1}^{\infty} k_m^i \left(\int_0^{d_i} \mathbf{N}_i^T(\xi_i) \chi_m^i(\xi_i) d\xi_i \right) \left(\int_0^{d_i} \mathbf{N}_i(\xi_i) \chi_m^i(\xi_i) d\xi_i \right) \mathbf{u}_i \right]. \end{aligned} \quad (42)$$

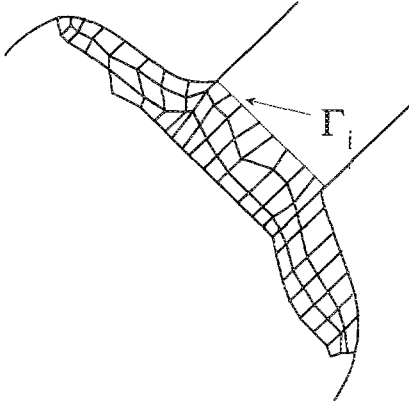


FIG. 3. Discretization of the interior region in the neighborhood of lead i .

Now using the definition of $\mathbf{N}_{i,m}$, we obtain,

$$\begin{aligned} \frac{\hbar^2}{2m^*} \sum_i \left(\int_{\Gamma_i} \bar{\psi}(\mathbf{r}) f_i(\mathbf{r}, \mathbf{u}) d\Gamma_i \right) \\ = \frac{\hbar^2}{2m^*} \sum_i \bar{\mathbf{u}}^T \\ \times \left[\sum_{m=1}^{N^i} -2ia_m^i k_m^i \mathbf{N}_{i,m}^T + \left(\sum_{m=1}^{N^i} ik_m^i \mathbf{N}_{i,m}^T \mathbf{N}_{i,m} \right) \mathbf{u}_i \right. \\ \left. - \left(\sum_{m=N^i+1}^{\infty} k_m^i \mathbf{N}_{i,m}^T \mathbf{N}_{i,m} \right) \mathbf{u}_i \right]. \end{aligned} \quad (43)$$

Define a vector \mathbf{P}_i and matrix \mathbf{C}_i as

$$\mathbf{P}_i \equiv -\frac{\hbar^2}{2m^*} \sum_{m=1}^{N^i} 2ia_m^i k_m^i \mathbf{N}_{i,m}^T \quad (44)$$

and

$$\begin{aligned} \mathbf{C}_i \equiv -\frac{\hbar^2}{2m^*} \sum_{m=1}^{N^i} ik_m^i \mathbf{N}_{i,m}^T \mathbf{N}_{i,m} \\ + \frac{\hbar^2}{2m^*} \sum_{m=N^i+1}^{\infty} k_m^i \mathbf{N}_{i,m}^T \mathbf{N}_{i,m}. \end{aligned} \quad (45)$$

The boundary term can then be written as

$$\sum_i \bar{\mathbf{u}}^T (\mathbf{P}_i - \mathbf{C}_i \mathbf{u}_i). \quad (46)$$

This can be further simplified if we define the embedded matrices $\hat{\mathbf{C}}$ and $\hat{\mathbf{P}}$ by

$$\sum_i \bar{\mathbf{u}}_i^T \mathbf{C}_i \mathbf{u}_i = \bar{\mathbf{u}}^T \hat{\mathbf{C}} \mathbf{u} \quad (47)$$

and

$$\sum_i \bar{\mathbf{u}}_i^T \mathbf{P}_i = \bar{\mathbf{u}}^T \hat{\mathbf{P}}. \quad (48)$$

The discretized Schrödinger equation then becomes

$$\bar{\mathbf{u}}^T (\mathbf{T} + \mathbf{V}) \mathbf{u} = \bar{\mathbf{u}}^T \hat{\mathbf{P}} - \bar{\mathbf{u}}^T \hat{\mathbf{C}} \mathbf{u} \quad (49)$$

or

$$\bar{\mathbf{u}}^T (\mathbf{T} + \mathbf{V} + \hat{\mathbf{C}}) \mathbf{u} = \bar{\mathbf{u}}^T \hat{\mathbf{P}}. \quad (50)$$

Since $\bar{\mathbf{u}}$ is arbitrary, this reduces to simply

$$(\mathbf{T} + \mathbf{V} + \hat{\mathbf{C}}) \mathbf{u} = \hat{\mathbf{P}}. \quad (51)$$

This is simply a set of m algebraic equations for the m un-

known nodal values of ψ in terms of the known quantities \mathbf{T} , \mathbf{V} , $\hat{\mathbf{C}}$, and $\hat{\mathbf{P}}$.

B. Algorithm summary

We summarize the numerical solution algorithm as follows.

(i) Discretize the device region Ω_0 on a mesh \mathbf{r}_i , $i = 1, 2, \dots, m$. The potential energy $V(x, y)$ should be known at least on these nodal points.

(ii) Choose a set of basis functions, $[\phi_i(x, y)]$, which obey Eq. (28).

(iii) Construct the $(m \times m)$ matrix \mathbf{T} using Eq. (37) or

$$T_{i,j} = \frac{\hbar^2}{2m^*} \int_{\Omega_0} [\partial_x \phi_i(\mathbf{r}) \partial_x \phi_j(\mathbf{r}) - \partial_y \phi_i(\mathbf{r}) \partial_y \phi_j(\mathbf{r})] d^2r. \quad (52)$$

(iv) Construct the $(m \times m)$ matrix \mathbf{V} using Eq. (38) or

$$V_{i,j} = \int_{\Omega_0} [V(\mathbf{r}) - E] \phi_i(\mathbf{r}) \phi_j(\mathbf{r}) d^2r. \quad (53)$$

(v) For each lead i , calculate the transverse eigenfunctions $\chi_m^i(\xi_i)$. Using the basis functions associated with M_i nodal points on the lead boundary Γ_i , calculate the vector $\mathbf{N}_{i,m}$ using Eq. (41).

(vi) Using $\mathbf{N}_{i,m}$, the given values of the a_m^i 's, and k_m^i 's from Eq. (14) calculate the M_i -by- M_i matrix \mathbf{C}_i and the vector \mathbf{P}_i for each lead using Eqs. (45) and (44). Embed these into the $(m \times m)$ matrix $\hat{\mathbf{C}}$ and the vector $\hat{\mathbf{P}}$ (this is usually done automatically in the assembly process).

(vii) Solve the system of linear equations

$$(\mathbf{T} + \mathbf{V} + \hat{\mathbf{C}}) \mathbf{u} = \hat{\mathbf{P}} \quad (54)$$

for the unknown nodal values of the wave function

$$u_j = \psi_0(\mathbf{r}_j). \quad (55)$$

Because $\mathbf{T} + \mathbf{V} + \hat{\mathbf{C}}$ is a sparse banded matrix, it is not necessary to store the entire $(m \times m)$ complex array. We have used both band-storage and profile-storage schemes. Solution routines are also available which take advantage of the sparse character of the matrix.⁷

(viii) From the calculated wave function, compute transmission coefficients, currents, or other quantities of interest.

Equation (45) contains an infinite sum over all possible evanescent modes. In practice this sum must be truncated to a value less than half the number of nodal points on the lead boundary. Usually a much smaller number of modes is sufficient for convergence. No general rule applies, however, because the number of evanescent modes excited depends on the details of $V(x, y)$ in the device region. If V varies rapidly, more evanescent modes need to be included in the sum.

C. Features of the algorithm

The principle features of the QTBM are as follows:

(i) The current-carrying states are solved for directly, yielding the wave function over the entire problem domain. Any other physical quantities of interest, e.g., the electron density, current distribution, or transmission coefficients, can then be extracted from the knowledge of the wave function. In particular, because the electron density is immedi-

ately available, extension of the method to include Poisson self-consistency should be straightforward.

(ii) Solution times are independent of the shape of $V(x, y)$ in the device region. Other than tabulating the values of the potential at nodal points, no additional computations are required to handle an arbitrary $V(x, y)$ than to handle a flat potential.

(iii) Multiple input and output leads are included naturally. Leads can have any size and extend away from the device region in any direction. Nonsquare-well leads are also handled simply.

(iv) For a device region with N_p nodal points, the algorithm requires the solution of one $2N_p \times 2N_p$ system of linear equations for the $2N_p$ unknown nodal values of the real and imaginary parts of the wave function.

(v) The algorithm is easy to implement using standard finite element programs. The current-carrying boundaries can be included as simply another element type. The new element subroutine associated with a boundary element computes \mathbf{C} and \mathbf{P} . The normal assembly process then performs the embedding of these into $\hat{\mathbf{C}}$ and $\hat{\mathbf{P}}$.

Presently, the most popular way of dealing with current-carrying states is to solve the Dyson equation on a tight-binding lattice for the real-space Green function.¹ This method is easiest to employ if the solution domains are very regular and the exact Green function is known in each of several connected regions. It is considerably more costly for arbitrary shapes and potentials. More important, it does not yield the wave function itself in the device region. The considerable physical insight which can be gained by having the full function is lost. Because of this, it may prove difficult to develop self-consistent solutions of the Schrödinger and Poisson equations. It should be noted that the Green function's may have an advantage in extending the current methods to include dissipation, techniques based on the Schrödinger equation will probably never be able to accomplish.

Recently Frohne, McLennan, and Datta developed a solution algorithm based on the boundary element method.⁸ Like the QTBM, this method is based on the real-space Schrödinger equation and yields the full wave function over the entire device domain. Its most important limitation is that it requires that the full set of eigenfunctions be known for a region which includes the device region, but may be larger and have more regular boundaries. It is particularly ill-equipped to handle variations of the potential within the device region, i.e., situations with $V(x, y) \neq 0$ over the device region because exact eigenfunctions are then difficult to obtain at the outset.

IV. EXAMPLES

We present two examples of the QTBM applied to fairly simple two-dimensional geometries. The first is a resonant cavity in a quantum waveguide. The geometry is illustrated in Fig. 4(b). For simplicity we assume here that the potential is zero inside the leads and in the interior of the cavity. Outside the leads and cavity the potential is taken to be infinite. The cavity has width W and length (in the direction of current flow) L . The width of both leads is d . The wave

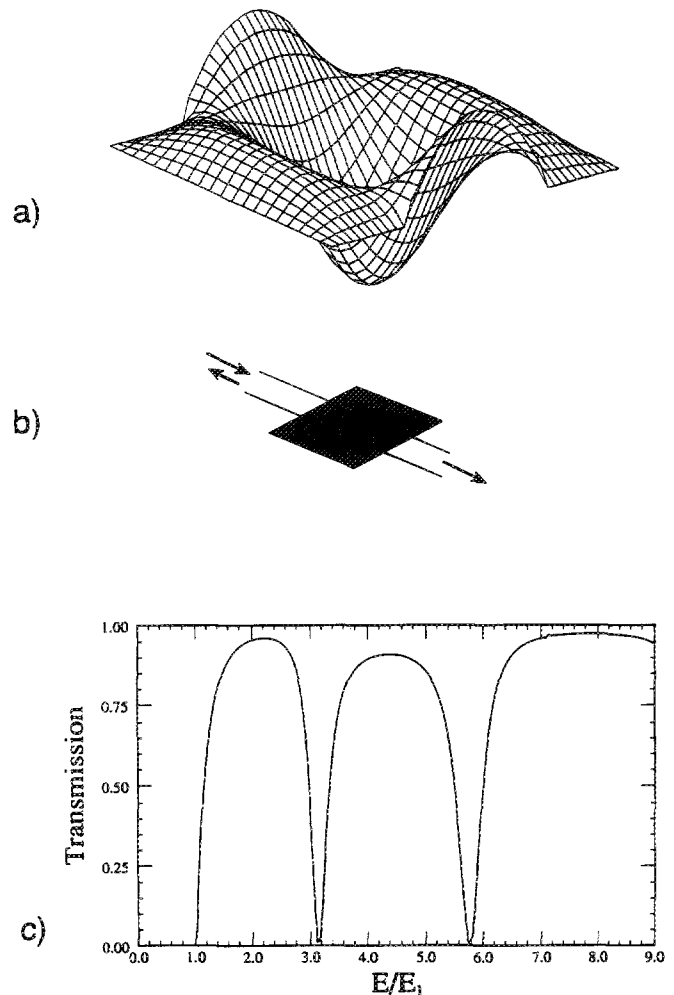


FIG. 4. Transmission through a rectangular cavity in a quantum waveguide. The real part of a typical wavefunction in a region with high transmission is shown in (a). The scattering geometry is shown in (b) which also illustrates the region (dark) over which the wave function is calculated. The transmission coefficient as a function of energy for the case of current incident in the lowest mode of the waveguide is shown in (c). The energy is normalized to E_1 , the minimum energy for traveling waves to exist in the leads.

function for a state with an incident wave coming from the left, in the lowest mode of the waveguide, is solved for over the region of the cavity (the device region in this case) for various values of the energy E . In this example we take $L/d = 1$ and $W/d = 2$. Figure 4(a) shows a typical wave function obtained from the QTBM calculation. The transmission coefficient as a function of energy is shown in Fig. 5(c). The energy scale is normalized to E_1 , the lowest transverse excitation of the waveguide. For energies lower the E_1 , only evanescent states can occur in the channel. The minima in the transmission coefficient occur near the energies of bound states of the cavity. Transmission maxima are also observed. A discussion of the precise nature of these resonances will be given elsewhere.⁹

As a second example we consider transmission through a circular arc in a quantum waveguide. This problem is of interest if true quantum-waveguide devices are to be connected in more than a linear arrangement. The width of the waveguide is d and the central radius of curvature is r .

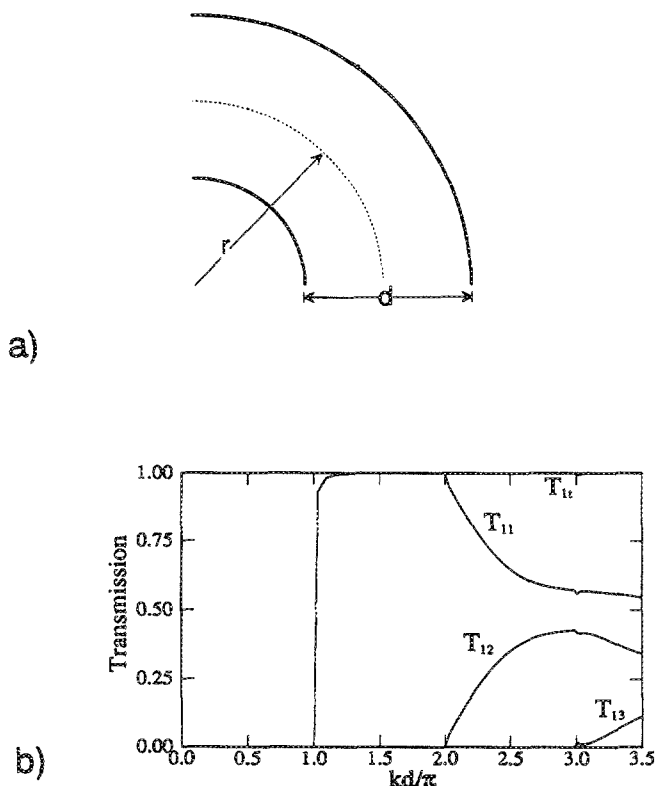


FIG. 5. A circular bend in a quantum channel. The geometry is shown in (a). The transmission coefficient for current incident in the lowest mode of the channel is displayed in (b) when $r/d = 0.7$. The transmission from the first mode into the first three modes is plotted vs kd/π where $k = \sqrt{2mE}/\hbar$.

Again, for simplicity the potential is assumed to be zero inside the waveguide and infinite outside. The arc is a full right-angle turn. The geometry of the waveguide is shown in Fig. 5(a). Unless the r is quite small the transmission is essentially unity for all values of the energy. However, the incoming wave in the first mode may be transmitted as a combination of higher-order modes. This mode mixing is the essential feature of such an arc. Figure 5(b) illustrates the mode-to-mode transmission coefficient $T_{i,j}$ for $i = 1$ (the incoming mode) and several outgoing modes when $r/d = 0.7$. This example illustrates the utility of the QTBM in

nonrectilinear geometries. The elements used in this calculation are not rectangular but are formed by generating a regular mesh in ρ and θ , the cylindrical coordinates natural for this problem.

Both the resonant cavity and the circular arc problems will be treated at greater length elsewhere.⁹ Transmission through a double cavity is discussed in Ref. 10. The examples here serve to illustrate the power of the QTBM approach. The circular arc geometry illustrates how easily nonrectilinear boundaries can be handled. In each case, a more complicated interior potential can easily be added.

V. CONCLUSIONS

We have developed a new technique for calculating numerically the solutions of the two-dimensional Schrödinger equation for current-carrying states. The quantum transmitting boundary method is based on our formulation of the boundary conditions appropriate for such states and an implementation of the finite element method. The technique is general enough to handle arbitrarily shaped device regions with complicated internal potentials. No *a priori* assumptions about the solution in the device region are required. Multiple contact leads with differing widths and various directions are handled naturally by the technique. We have demonstrated its utility in two cases of interest for quantum-waveguide devices.

¹F. Sols, M. Macucci, U. Ravaioli, and K. Hess, *Appl. Phys. Lett.* **54**, 350 (1989).

²S. Datta, *Superlattices Microstructures* **6**, 83 (1989).

³M. Heiblum and C. Umbach, in *Nanostructure Physics and Fabrication*, edited by M. A. Reed and W. P. Kirk (Academic, Boston, 1989).

⁴A. M. Kriman, G. H. Bernstein, B. S. Haukness, and D. K. Ferry, *Superlattices Microstructures* (in press).

⁵G. Bernstein and D. K. Ferry, *J. Vac. Sci. Technol. B* **5**, 964 (1987).

⁶David J. Kirkner and Craig S. Lent, *International Journal of Numerical Methods in Engineering* (in press).

⁷T. J. R. Hughes, *The Finite Element Method* (Prentice Hall, Englewood Cliffs, NJ, 1987).

⁸H. Rob Frohne, M. J. McLennan, and S. Datta, *J. Appl. Phys.* **66**, 2699 (1989).

⁹C. S. Lent and S. Sivaprakasam (unpublished).

¹⁰C. S. Lent, S. Sivaprakasam, and D. J. Kirkner, in *Nanostructure Physics and Fabrication*, edited by M. A. Reed and W. P. Kirk (Academic, Boston, 1989).